Arabidopsis *IAR4* Modulates Auxin Response by Regulating Auxin Homeostasis[1][OA]

Marcel Quint[2], Lana S. Barkawi, Kai-Ting Fan, Jerry D. Cohen, and William M. Gray*

Department of Plant Biology (M.Q., K.-T.F., W.M.G.) and Department of Horticultural Sciences (L.S.B., J.D.C.), University of Minnesota, St. Paul, Minnesota 55108

In a screen for enhancers of *tir1-1* auxin resistance, we identified two novel alleles of the putative mitochondrial pyruvate dehydrogenase E1α-subunit, *IAA-Alanine Resistant4* (*IAR4*). In addition to enhancing the auxin response defects of *tir1-1*, *iar4* single mutants exhibit numerous auxin-related phenotypes including auxin-resistant root growth and reduced lateral root development, as well as defects in primary root growth, root hair initiation, and root hair elongation. Remarkably, all of these *iar4* mutant phenotypes were rescued when endogenous indole-3-acetic acid (IAA) levels were increased by growth at high temperature or overexpression of the YUCCA1 IAA biosynthetic enzyme, suggesting that *iar4* mutations may alter IAA homeostasis rather than auxin response. Consistent with this possibility, *iar4* mutants exhibit increased Aux/IAA stability compared to wild type under basal conditions, but not in response to an auxin treatment. Measurements of free IAA levels detected no significant difference between *iar4-3* and wild-type controls. However, we consistently observed significantly higher levels of IAA-amino acid conjugates in the *iar4-3* mutant. Furthermore, using stable isotope-labeled IAA precursors, we observed a significant increase in the relative utilization of the Trp-independent IAA biosynthetic pathway in *iar4-3*. We therefore suggest that the auxin phenotypes of *iar4* mutants are the result of altered IAA homeostasis.

Auxin regulates numerous aspects of plant development and physiology, including embryogenesis, vascular differentiation, organogenesis, tropic growth, and root and shoot architecture. In a simplified view, auxin biology can be broken down into three general areas: indole-3-acetic acid (IAA) biosynthesis and metabolism, the cell-to-cell transport of IAA, and the SCF^{TIR1}-mediated signaling events leading to an auxin response. Despite several recent advances, perhaps the least understood of these three areas is auxin biosynthesis and metabolism. Several redundant biosynthetic routes seem to coexist and ultimately result in the synthesis of the major biologically active auxin in plants, IAA (Woodward and Bartel, 2005). These pathways differ in their dependence upon the IAA precursor Trp and can therefore be distinguished as Trp-dependent and Trp-independent pathways (Cohen et al., 2003). IAA metabolism, namely the biology of its conjugates, is regulated by IAA-conjugating and IAA-hydrolyzing enzymes that either conjugate free IAA to sugars, amino acids, and proteins or release it from these compounds back into the biologically active free IAA pool (Ljung et al., 2002; Walz et al., 2002).

Once synthesized, a complex system of auxin influx and efflux carriers (Kramer and Bennett, 2006) transports the hormone to its target cells where it is perceived by the nuclear-localized TIR1/auxin F-box (AFB) family of receptors, triggering the SCF$^{TIR1/AFB}$-mediated ubiquitylation of Aux/IAA proteins (Gray et al., 2001; Dharmasiri et al., 2005). Subsequent degradation of these transcriptional repressors results in changes in auxin-regulated gene expression and corresponding changes in plant growth and development (Quint and Gray, 2006).

Thus, a proper auxin response is dependent upon adequate levels of free IAA, and the delivery of that IAA to the responding cells. While considerable progress on how the separate processes of IAA metabolism, transport, and signaling has been achieved in recent years, the integration of these pathways is only beginning to be understood. The auxin induction of the expression of several IAA-conjugating enzymes encoded by *GH3* genes (Staswick et al., 2005), as well as the repression of IAA biosynthetic enzymes (Goddijn et al., 1992) are examples of feedback regulation of the response pathway on IAA metabolism. Likewise, auxin has been shown to regulate the abundance and polarity of members of the PIN family of auxin efflux proteins, indicating connections between the signaling and transport pathways (Paciorek et al., 2005; Abas et al., 2006; Sauer et al., 2006).

LeClere et al. (2004) and colleagues identified mutations in the Arabidopsis (*Arabidopsis thaliana*) *IAA-Alanine Resistant4* (*IAR4*) gene in a mutant screen for seedlings resistant to IAA-Ala and other IAA-amino

acid conjugates. *IAR4* encodes a putative mitochondrial E1α pyruvate dehydrogenase subunit; however, its role in the auxin pathway is unclear. LeClere et al. (2004) speculated that IAR4 may be involved in IAA metabolism, perhaps by catalyzing the conversion of indole-3-pyruvate (IPA) to IAA-CoA. However, no further studies examining this or other potential roles for IAR4 in auxin metabolism have been reported. We identified two additional *IAR4* alleles in a screen for mutations that enhance the weak auxin response defect conferred by the Arabidopsis *tir1-1* mutation. We find that while *iar4* mutants exhibit several phenotypes consistent with reduced auxin response, these phenotypes can be suppressed by increasing endogenous IAA levels. Here we report our efforts to understand the role of *IAR4* in the auxin pathway and demonstrate that *iar4* mutants exhibit defects in IAA homeostasis rather than auxin signal transduction per se. Specifically, we find that *iar4* mutants accumulate IAA-amino acid conjugates and exhibit altered IAA biosynthesis pathway utilization.

RESULTS

Identification of the *eta5* Mutation

With the aim of identifying additional components of the SCF^{TIR1}-mediated auxin response pathway, we have previously performed a genetic screen to isolate *enhancers of tir1-1 auxin* (*eta*) resistance. This screen identified mutations in several loci that are directly involved in the regulation of the SCF^{TIR1} complex, including *ETA1/CUL1* (Quint et al., 2005), *ETA2/CAND1* (Chuang et al., 2004), *ETA3/SGT1b* (Gray et al., 2003), and *ETA6/CSN1/FUS6* (Zhang et al., 2008). We also identified two recessive, allelic muta-tions, designated *eta5-1* and *eta5-2*. Analysis of the F2 progeny from Columbia (Col) backcrosses revealed that *eta5* single mutants were resistant to low concentrations of exogenous auxins (Fig. 1A). Also consistent with reduced auxin response, *eta5* seedlings developed fewer lateral roots than the wild type on unsupplemented nutrient medium (Fig. 1B). As expected, both defects were exacerbated in the *eta5*, *tir1-1* double mutants. While adult *eta5* mutants look similar to wild-type plants, the mutant seedlings exhibit several root growth defects. In addition to reduced lateral root development, *eta5* primary roots are shorter than wild type (Fig. 1C) and develop both fewer and shorter root hairs (Fig. 1, D–F). Auxin is known to control both root hair initiation and elongation (Masucci and Schiefelbein, 1996).

ETA5 Is Allelic to IAR4

A map-based cloning approach was used to isolate the *ETA5* gene. Linkage studies placed the *eta5* mutations within an approximately 117-kb interval on chromosome 1. Among the genes in this region was *IAR4* (AT1G24180), encoding a putative mitochondrial pyruvate dehydrogenase E1α-subunit. The pyruvate dehydrogenase complex (PDC) catalyzes the oxidative decarboxylation of pyruvate and the subsequent acetylation of coenzyme A to acetyl-CoA (Mooney et al., 2002). The E1 component of the PDC catalyzes the first step of this process. In mitochondria, this reaction represents the irreversible commitment of carbon to the tricitric acid cycle. Thus, *IAR4* presumably encodes a subunit of an important metabolic enzyme. Mutations in *IAR4* were recently identified in a screen for mutants resistant to IAA-Ala conjugates (LeClere et al., 2004). We therefore sequenced the *IAR4* locus in both of our *eta5* mutants. *eta5-1* possesses a non-
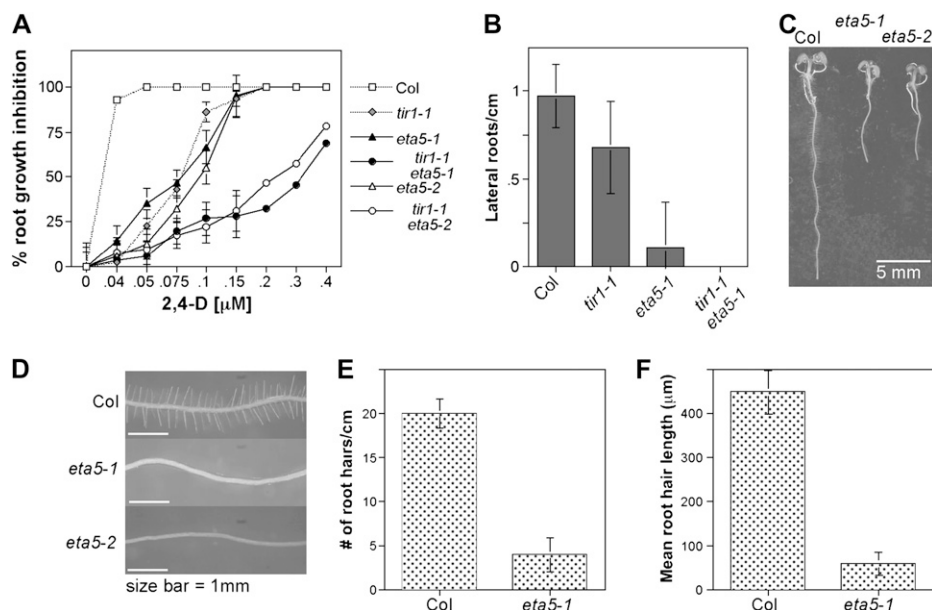

Figure 1. *eta5* mutants exhibit defects in auxin-regulated pathways. A, Inhibition of root elongation by increasing concentrations of the synthetic auxin 2,4-D. Five-day-old seedlings grown on ATS were transferred to medium containing 2,4-D and grown three additional days (*n* = 10). B, Lateral root initiation was assessed in 10-d-old seedlings grown on unsupplemented ATS nutrient medium. C, Six-day-old seedlings grown on unsupplemented ATS medium. D, Root hairs in the maturation zone of 6-d-old seedlings. E, Number of root hairs per centimeter for 6-d-old seedlings in the maturation zone of the primary root (*n* = 25). F, Length of root hairs of 6-d-old seedlings in the maturation zone of the primary root (*n* = 100). All assays were conducted at 20°C. Error bars indicate SD from the mean.

sense mutation near the end of the first exon ($G^{653}A$), while *eta5-2* contains a single base-pair change at the extreme 3′ end of the fifth intron ($G^{2378}A$; Fig. 2A). Further confirmation that the *eta5* mutations are allelic with *IAR4* was obtained by complementation tests with the previously described *iar4-2* T-DNA allele (LeClere et al., 2004; data not shown). We therefore renamed the *eta5-1* and *eta5-2* mutants as *iar4-3* and *iar4-4*, respectively. Like the previously described *iar4* alleles, *iar4-3* and *iar4-4* exhibit resistance to IAA-Ala in root growth assays (data not shown).

To examine *IAR4* expression patterns, we generated transgenic plants expressing an *IAR4* promoter-GUS reporter construct. In agreement with publicly available microarray datasets, we find that *IAR4* is expressed throughout the plant. Consistent with the observed root phenotypes, *IAR4* is strongly expressed in roots, with highest expression detected at the root tip (Fig. 2B). Auxin treatment did not appear to affect the level or pattern of expression (data not shown). The predicted role of IAR4 as a PDC E1α-subunit and putative mitochondrial targeting sequence suggested that IAR4 is a mitochondrial protein. To test this possibility, we fused GFP to the C terminus of the IAR4 coding sequence and expressed this fusion protein from the *IAR4* promoter. Like the P*IAR4*-GUS reporter, IAR4:GFP was expressed most strongly in roots. GFP fluorescence colocalized with a mitochondrial stain, confirming the predicted cellular compartmentalization (Fig. 2C). No nuclear localization, as it would be expected for a function in auxin signaling, could be detected.

IAR4 Exhibits Partial Redundancy with the Closely Related *IAR4L* Gene

The Arabidopsis genome encodes three apparent PDC E1α-subunits. The previously characterized PDC E1α-subunit encoded by At1g01090 carries a plastidic signature and is 32% identical to IAR4 on the amino acid level (Johnston et al., 1997). IAR4 and the previously described At1g59900 (designated here as IAR4-LIKE [IAR4L]) proteins display a mitochondrial targeting sequence and are 81% identical (Luethy et al., 1995). LeClere et al. (2004) examined *iar4* mutants for phenotypes consistent with respiratory pathway defects, but found no differences from wild type on media containing various concentrations of Suc, citrate, or ethanol. These findings could be the result of functional redundancy between *IAR4* and *IAR4L*; however, it also raises the possibility that *IAR4* has evolved an auxin-specific function. LeClere et al.

Figure 2. *eta5-1* and *eta5-2* are novel alleles of *IAR4*. A, Exon-intron structure of *IAR4*. B, *IAR4*pro:GUS expression in 6-d-old seedlings, rosette leaf, and flower. C, Confocal microscopic images of IAR4pro:IAR4:GFP in various tissues (top). The IAR4-GFP fusion protein localizes to the mitochondria in root hairs (bottom).
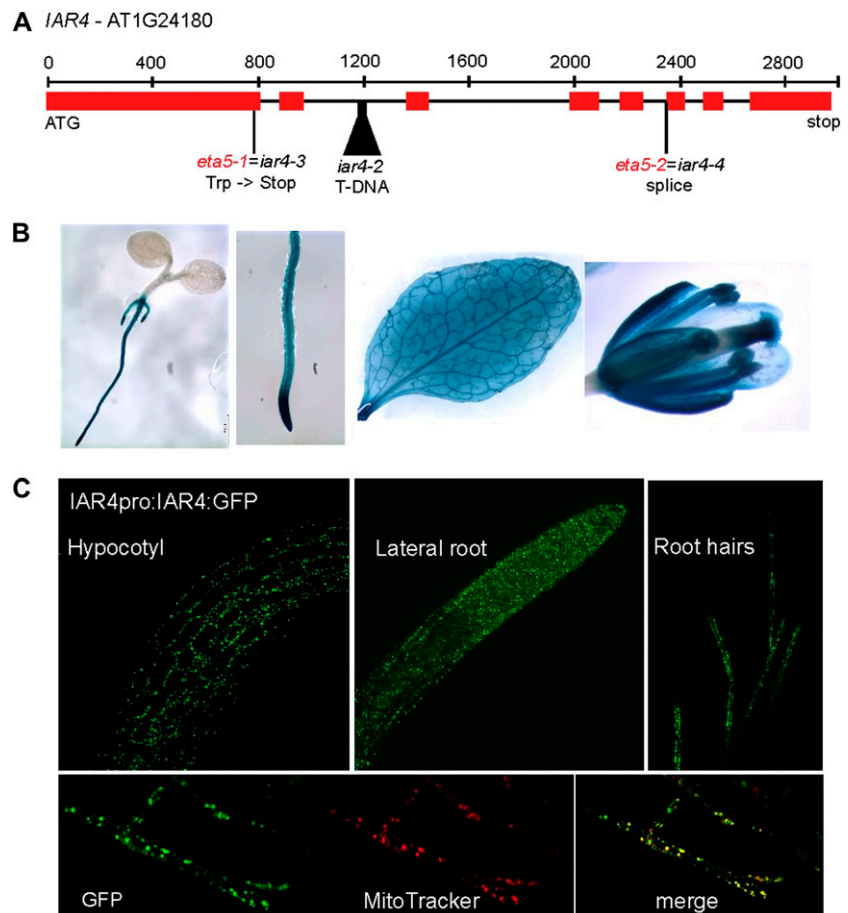
(2004) reported that the *iar4L-1* T-DNA (SALK_074384) mutant displayed wild-type sensitivity to IAA-Ala and other auxins. In agreement with these findings we could not detect any auxin-related defects in *iar4L-1* seedlings such as we observe with *iar4* mutants (data not shown).

To examine the possibility that *IAR4* and *IAR4L* functionally overlap, we crossed *iar4-3* with *iar4L*. No double mutant progeny were recovered in the F2 generation, suggesting embryo and/or gametophyte lethality. Furthermore, when *iar4-3* homozygous F2 plants were PCR genotyped for *IAR4L*, we found that none of these plants (0/28) carried the *iar4L-1* T-DNA allele. In contrast, we did identify *iar4L-1* homozygotes that were heterozygous for *iar4-3*; however, no *iar4-3* homozygotes were detected in the F3 progeny of these plants. We examined the embryos in the siliques of the *iar4L-1/iar4L-1 iar4-3/+* plants, but observed no aborted embryos, suggesting that the double mutant may be gametophyte lethal.

In the F2 populations of our backcrosses of *iar4-3* to Col we consistently observed a modest but significant deviation from a 3:1 segregation ratio (Table I), suggesting reduced transmission of *iar4-3* gametes. This reduction in the recovery of *iar4-3* homozygotes was dramatically more severe in the F2 populations of *iar4-3* × *iar4L-1* (Table I). To investigate the basis of the reduced transmission of *iar4-3*, we conducted reciprocal crosses with *IAR4/iar4-3* heterozygous plants. A significant reduction in transmission through the pollen was detected (Table I). We therefore considered the possibility that our failure to recover *iar4L-1 iar4-3* double mutants might be the result of *iar4L* enhancing the reduced pollen transmission phenotype of *iar4-3*. When *iar4L-1/iar4L-1 iar4-3/+* plants were reciprocally crossed with Col, we observed a complete lack of transmission of *iar4-3* through pollen. In contrast, transmission rates through the female gametes were normal (Table I). To elucidate why *iar4L-1 iar4-3* pollen was not transmitted, we used Alexander's stain to determine whether or not the pollen was viable. While pollen obtained from Col, *iar4-3*, and *iar4L-1* flowers were virtually 100% viable, only approximately 50% (385/788) of the pollen from *iar4L-1/iar4L-1 iar4-3/+*

plants was viable (Fig. 3A), indicating that *iar4L-1 iar4-3* is pollen lethal.

While our finding that *iar4L-1 iar4-3* pollen is inviable explained our inability to recover double mutant plants, it could not account for our failure to isolate *iar4L-1/+*, *iar4-3/iar4-3* plants in the F2 progeny of the cross between the two single mutants. We therefore considered the possibility that this genotype confers an embryo-lethal phenotype. To test this possibility, we used *iar4-3* pollen to fertilize *iar4L-1/iar4L-1*, *iar4-3/+* flowers. The resulting progeny should either be heterozygous for both genes or homozygous for *iar4-3* and heterozygous for *iar4L-1*. However, none of the progeny exhibited the *iar4-3* mutant phenotype. We then repeated this cross and examined the developing F1 embryos within the siliques. When examined 6 d after pollination, nearly all of the embryos from *IAR4*-pollinated flowers were at the heart stage. In contrast, when *iar4-3* was used as the pollen donor, two distinct classes of embryos were observed with equal frequency: heart stage embryos similar to the *IAR4* control, and small globular embryos (Fig. 3B). When examined at later stages of development, the globular embryos had failed to progress, indicating a developmental arrest (Fig. 3C). Consistent with this possibility, approximately half of the seeds obtained from the *iar4-3* crosses were shriveled and failed to germinate (Fig. 3D). Thus, in addition to an essential role in pollen development, *IAR4* is also essential for embryogenesis in plants with reduced dosage of *IAR4L*.

## *iar4* Specifically Affects Basal Aux/IAA Protein Stability

To further characterize the auxin response of *iar4* mutants, SCF^{TIR1} activity was examined by introducing the HS::AXR3NT-GUS reporter construct to examine Aux/IAA protein stability (Gray et al., 2001). Wild-type and *iar4-3* seedlings containing the reporter were heat shocked to induce expression of the transgene, incubated at room temperature in the absence or presence of exogenous auxin, and subsequently stained for GUS expression. To examine the basal level of the AXR3NT-GUS fusion protein, the seedlings were GUS stained immediately after the heat-shock

Table I. *Inheritance of iar4-3 in IAR4L and iar4L-1 backgrounds*

	2,4-D Sensitive	2,4-D Resistant	χ^2 Value
Col × *iar4-3*; F2	242	60	4.24[a] (3:1)
iar4-3 × *iar4L-1*; F2	238	28	29.7[a] (3:1)
IAR4/iar 4-3 ♀ × *iar4-3* ♂; F1	64	68	0.12 (1:1)
iar4-3 ♀ × *IAR4/iar4-3* ♂; F1	191	131	11.2[a] (1:1)
iar4L-1/iar4L-1 IAR4/iar4-3 ♀ × *Col* ♂	18	22[b]	0.4 (1:1)
Col ♀ × *iar4L-1/iar4L-1 IAR4/iar4-3* ♂	44	0[b]	44[a] (1:1)

[a]Significant deviation from expected using a 5% critical value.   [b]*iar4-3* transmission was assessed by the appearance of 2,4-D-resistant F2 segregants. Numbers correspond to the number of F1 plants that segregated *iar4-3/iar4-3* 2,4-D-resistant progeny.

Figure 3. Genetic interactions between *IAR4* and *IAR4L*. A, Alexander's staining of pollen viability. B and C, Visualization of the two classes of embryos obtained in crosses between *iar4L/iar4L IAR4/iar4-3* and *iar4-3*. Embryos were examined at 6 and 14 d after pollination (d.a.p.). D, Underdeveloped seeds are present in the siliques obtained from crosses between *iar4L/iar4L IAR4/iar4-3* and *iar4-3* plants.
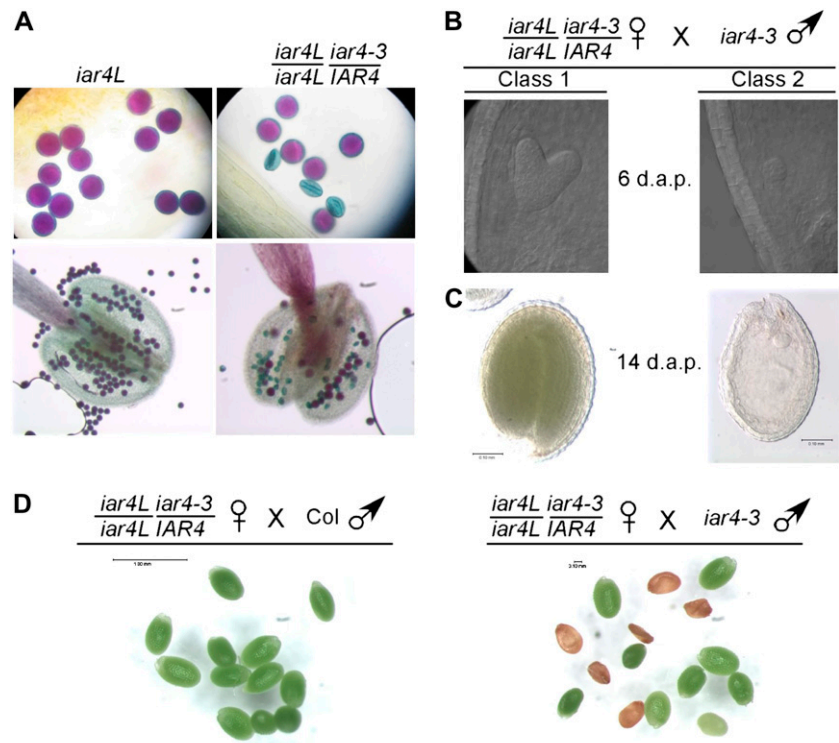
period. Surprisingly, *iar4-3* seedlings exhibited dramatically higher levels of AXR3NT-GUS staining (Fig. 4A). To better assess decay rates of the reporter protein, different staining times for GUS activity were subsequently used for wild-type and mutant seedlings such that staining intensities at time zero were equivalent. In the absence of exogenous auxin, *iar4-3* seedlings exhibited an obvious increase in AXR3NT-GUS stability, suggesting that SCF^{TIR1} activity is impaired (Fig. 4B). Surprisingly however, when the assay was performed in auxin-supplemented medium, wild-type and *iar4-3* seedlings exhibited comparable AXR3NT-GUS degradation kinetics (Fig. 4C).

The finding that the AXR3NT-GUS reporter responded normally to applied auxin in *iar4-3* seedlings raised the possibility that the differences we observed on unsupplemented medium may be due to a reduction in endogenous IAA levels rather than diminished SCF^{TIR1} function. To begin to address this possibility, wild-type and *iar4-3* seedlings containing the HS::AXR3NT-GUS reporter were grown at 28°C—a growth condition previously shown to increase endogenous IAA levels (Gray et al., 1998). When shifted to 28°C 2 d prior to staining, *iar4-3* seedlings exhibited no difference from wild-type controls for AXR3NT-GUS expression (Fig. 4D). Auxin-induced gene expression involves the auxin-dependent SCF^{TIR1}-mediated ubiquitination of Aux/IAA proteins, resulting in derepression of auxin response factor transcription factors (Quint and Gray, 2006). Our findings with the HS::AXR3NT-GUS reporter suggested that Aux/IAA proteins are stabilized in *iar4-3* seedlings grown at 20°C on unsupplemented medium. However, both exogenous auxin and increasing endogenous IAA levels by growth at high temperature restored AXR3NT-GUS levels to that seen in wild-type controls. These results are consistent with the possibility that SCF^{TIR1} activity per se is not affected in *iar4-3*, but rather that auxin levels are diminished in this mutant, resulting in less-efficient targeting of the AXR3NT-GUS fusion protein to the SCF^{TIR1} complex. To explore this possibility further, we examined the effect of *iar4* mutations on auxin-induced gene expression using the DR5::GUS reporter construct. When grown at 20°C, *iar4-3* seedlings exhibit a dramatic decrease in DR5::GUS expression in root tips of 6-d-old seedlings (Fig. 4E). However, when grown at 28°C, DR5::GUS expression in *iar4-3* was largely restored to wild-type levels (Fig. 4F).

Rescuing *iar4-3* Defects by Increasing Endogenous IAA Levels

The finding that high-temperature growth suppresses the defects in both DR5::GUS expression and AXR3NT-GUS degradation of *iar4-3* mutants led us to test whether other aspects of the mutant phenotype could be suppressed by increasing endogenous IAA levels. Growth at high temperature completely rescued the *iar4-3* defects in 2,4-dichlorophenoxyacetic acid (2,4-D) response, lateral root development, and root hair initiation, and partially rescued the root hair elongation and root growth phenotypes (Fig. 5, A–C). Likewise, incubation at high temperature also suppressed *iar4-4* as well as the *iar4-2* T-DNA allele (Fig.
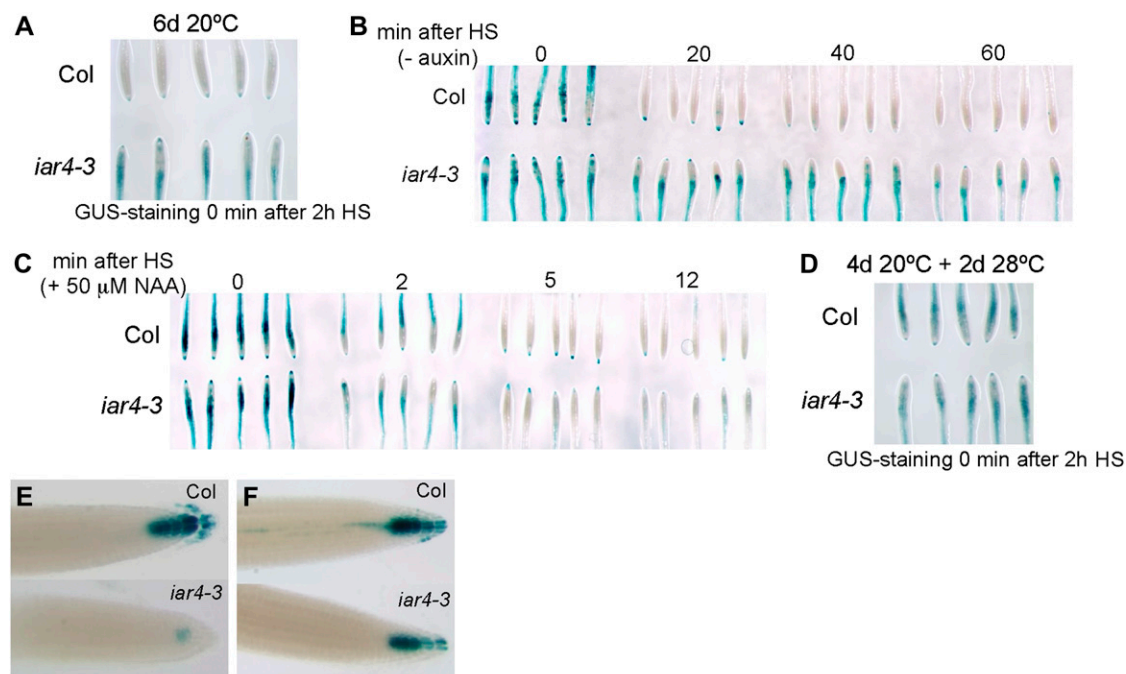
Figure 4. *iar4-3* plants exhibit Aux/IAA stabilization only under basal conditions. A, Col and *iar4-3* seedlings carrying the HS::AXR3NT-GUS transgene were grown for 6 d at 20°C and subsequently heat shocked for 2 h to induce expression of the AXR3NT-GUS fusion protein. Seedlings were briefly (50 min) stained for GUS activity immediately after the heat-shock (HS) period. B, Col and *iar4-3* seedlings carrying the HS::AXR3NT-GUS transgene were grown for 6 d at 20°C, heat shocked to induce expression of the transgene, and stained for GUS activity immediately, or following a 20-, 40-, or 60-min incubation at room temperature in ATS medium. C, Following a 2-, 5-, or 12-min incubation in ATS medium containing 50 μM 1-naphthaleneacetic acid. Seedlings in A were stained for 50 min. To account for the difference in AXR3NT-GUS levels and obtain a similar staining baseline for the degradation assay, Col and *iar4-3* seedlings were stained for different lengths of time in B and C. See "Materials and Methods" for details. D, Col and *iar4-3* seedlings carrying the HS::AXR3NT-GUS transgene were shifted to 28°C for 2 d and then heat shocked for 2 h to induce expression of the AXR3NT-GUS fusion protein. Seedlings were stained 8 h for GUS activity immediately after the heat-shock period. E, DR5::GUS expression of 6-d-old seedlings grown at 20°C on ATS medium. F, DR5::GUS expression of 6-d-old seedlings that were shifted to 28°C for 3 d prior to staining. Equivalent staining times were used for the seedlings shown in E and F.

5C; data not shown), indicating that suppression was not allele specific. To test the possibility that the effects of temperature on the *iar4-3* phenotypes were due to something other than elevated IAA levels, we introduced the *35S::YUCCA* transgene into *iar4-3* plants. YUCCA catalyzes a rate-limiting step in the Trp-dependent IAA biosynthetic pathway, and the activation-tagged *35S::YUC* transgene confers a significant increase in endogenous IAA levels compared to wild type (Zhao et al., 2001). Like the high-temperature studies, the *35S::YUC* transgene completely or partially rescued the *iar4-3* mutant phenotypes (Fig. 5, A–C).

Mutations in *IAR4* Affect Auxin Biosynthesis and Metabolism

A simple explanation for the above results is that *iar4* mutations confer a reduction in free IAA levels. IAA is known to regulate seedling hypocotyl length. Auxin overproducers such as *35S:YUC* (Zhao et al., 2001) and *sur2-1* (Delarue et al., 1998) exhibit a long

hypocotyl phenotype, while *35S::iaaL* seedlings, which contain reduced free IAA content, have shorter hypocotyls than wild type (Gray et al., 1998). Consistent with the possibility that *iar4* seedlings are IAA deficient, *iar4-3* seedlings have significantly shorter hypocotyls than wild type (Fig. 6A). Again, high temperature and the *35S::YUC* transgene completely suppressed this defect (Fig. 6, A and B).

Measurement of free IAA levels in whole seedlings, as well as root and shoot tissues separately, failed to detect a significant difference between wild type and *iar4-3* (Fig. 6C). To further examine possible effects of the *iar4-3* mutation on IAA biosynthesis, we compared the utilization of Trp and Trp-independent IAA biosynthetic pathways. Wild-type and *iar4-3* seedlings were fed the stable isotope-labeled IAA precursors [15N]anthranilic acid and [2H5]Trp, and the relative incorporation of these precursors into the free IAA pool was determined. In current IAA biosynthesis models, anthranilic acid is believed to be upstream and Trp downstream of the divergence point of the Trp-dependent and Trp-independent pathways (Fig.

Figure 5. Increasing endogenous auxin levels rescues the defects in *iar4-3*. A, Five-day-old seedlings grown on ATS medium at indicated temperature were transferred to medium containing 0.05 μM 2,4-D and grown three additional days ($n = 10$). White lines indicate positions of the root tip at the time of transfer. B, Lateral root initiation was assessed in 10-d-old seedlings grown on unsupplemented ATS nutrient medium at indicated temperature ($n = 10$). C, Number of root hairs per cm ($n = 25$) and root hair length ($n = 100$) for 6-d-old seedlings in the maturation zone of the primary root at indicated temperatures. Error bars indicate SD from the mean.
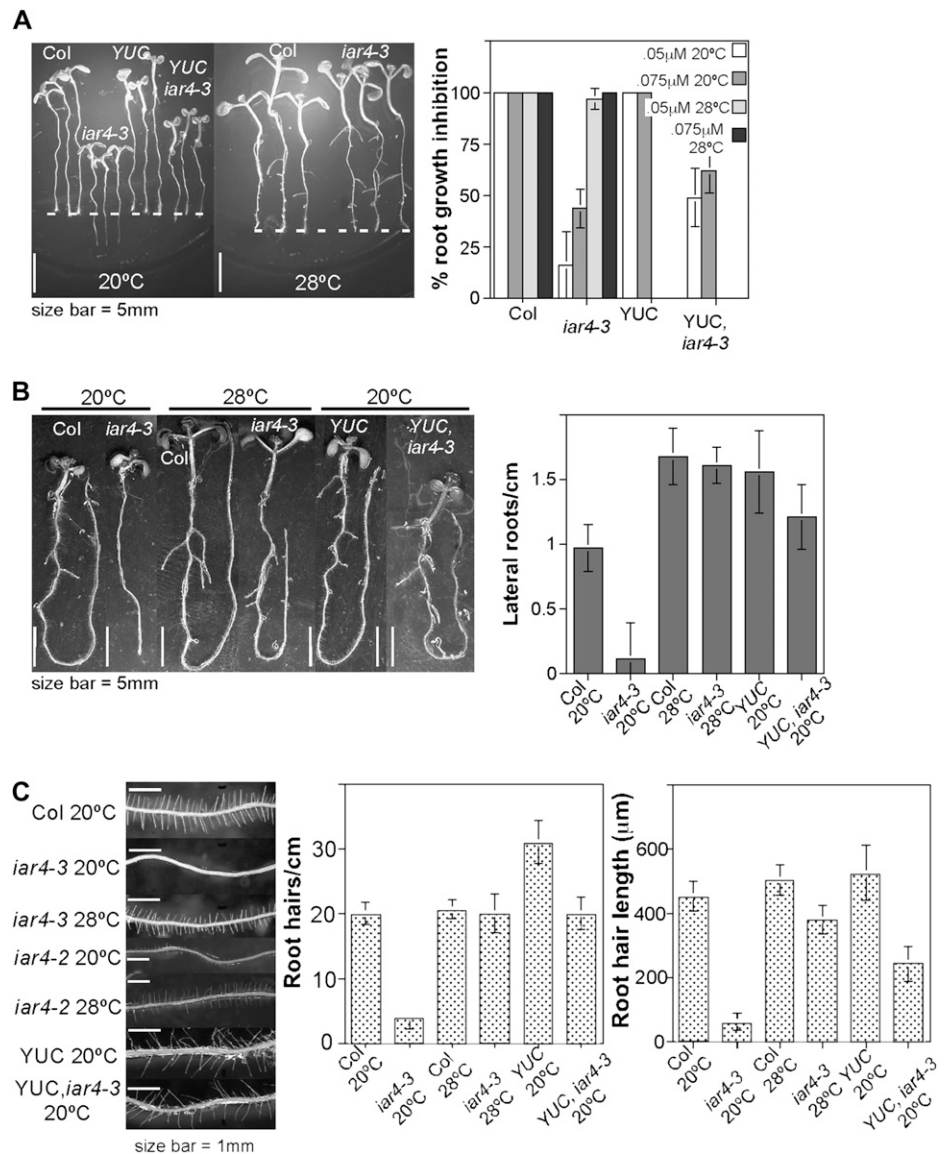
6D). The ratio of the two isotopes within the free IAA pool therefore allows the relative utilization of each pathway to be assessed (Rapparini et al., 2002). Compared to wild-type 10-d-old seedlings, the *iar4-3* mutant exhibited a significant increase in the utilization of the Trp-independent pathway (Fig. 6E), demonstrating that the *iar4-3* mutation does alter IAA biosynthesis.

Lastly, we also examined IAA conjugate levels in *iar4-3* mutant seedlings. Two distinct classes of IAA conjugates have been described in a variety of plant species. Ester conjugates, where the carboxyl group of IAA is linked to sugars or cyclic poly-ols like Glc and inositol, and amide conjugates with amino acids or polypeptides (Ljung et al., 2002). Measurement of IAA conjugate levels in wild-type and the *iar4-3* mutant revealed no differences in IAA-ester or IAA-protein conjugates (data not shown). However, *iar4-3* seedlings exhibited an approximately 2-fold increase in

IAA-amino acid conjugate abundance (Fig. 6F). To examine the effects of *iar4-3* on specific IAA-amino acid conjugates, we examined levels of IAA-Asp and IAA-Glu. We detected a significant increase in IAA-Glu, but not IAA-Asp levels in *iar4-3* seedlings, suggesting some specificity in the role of IAR4 in the regulation of IAA conjugates (Fig. 6G).

DISCUSSION

In the past 20 years, several mutants exhibiting altered auxin sensitivity have been described, most of which affect the SCF$^{TIR1/AFB}$ signal transduction pathway (Quint and Gray, 2006). In a genetic screen to identify additional factors involved in auxin signaling in Arabidopsis, we identified two novel alleles of *IAR4*, which encodes a putative E1α-subunit of the mitochondrial PDC. While *iar4* mutants exhibit several
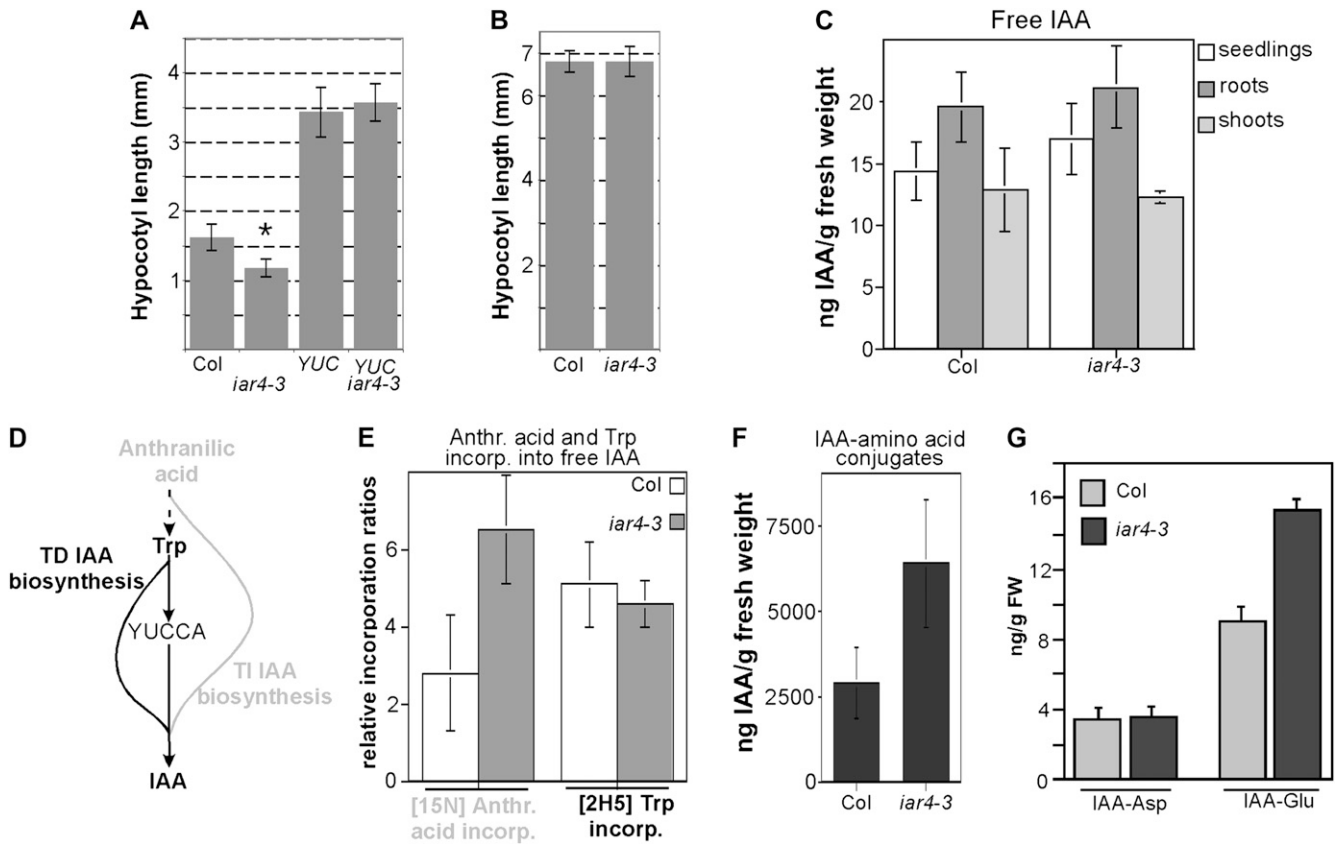
Figure 6. Pattern of IAA biosynthesis and metabolism. A, Hypocotyl length of 7-d-old seedlings grown at 20°C on ATS medium ($n = 10$). Asterisk indicates significant difference from Col control ($P < 0.05$). B, Hypocotyl length of 7-d-old seedlings grown at 28°C on ATS medium ($n = 10$). C, Free IAA levels of 10-d-old seedlings grown at 20°C on ATS medium ($n = 4$). D, Trp-dependent (TD) and Trp-independent (TI) IAA biosynthesis pathways. E, Incorporation of stable-isotope labeled IAA precursors [^{15}N]anthranilate and [^{2}H$_5$]Trp into the free IAA pool. Seedlings were grown for 10 d on ATS plates at 20°C prior to adding the labeled feeding solution for 24 h ($n = 4$). F, IAA-amino acid conjugates of 10-d-old seedlings grown on ATS medium at 20°C ($n = 4$). G, IAA-Asp and IAA-Glu conjugate levels in 10-d-old seedlings ($n = 3$). Error bars indicate SD from the mean.

phenotypes consistent with diminished auxin response phenotypes, including reduced lateral root development, short hypocotyls, and diminished root hair initiation and elongation, our findings suggest that *IAR4* functions in auxin homeostasis rather than auxin signaling.

We find that nearly all *iar4* mutant phenotypes can be completely or partially suppressed by elevating endogenous auxin levels through either high-temperature growth or introduction of the 35S::*YUCCA* transgene. These findings suggest that *iar4* phenotypes are the result of auxin deficiency. In response to auxin, the SCF$^{TIR1/AFB}$ ubiquitin ligases target Aux/IAA proteins for ubiquitin-mediated proteolysis, thus derepressing the expression of auxin-regulated genes. Our studies with the HS::AXR3NT-GUS reporter indicate that mutation of *iar4* leads to increased Aux/IAA stability when only endogenous auxin is present. Like the *iar4* growth phenotypes, however, this defect is suppressed by high-temperature growth or by supplementing the media with exogenous auxin. This behavior is

consistent with the notion that SCF$^{TIR1/AFB}$ activity per se is unaffected in *iar4* mutants, and that the increased AXR3NT-GUS stability we observe with unsupplemented *iar4* seedlings is the result of diminished endogenous IAA levels, resulting in reduced targeting of Aux/IAA proteins to the SCF$^{TIR1/AFB}$ complex.

While the above findings suggest that *iar4* mutants suffer from IAA deficiency, we were unable to detect a significant reduction in free IAA content at the whole seedling level or within isolated roots and shoots. It remains possible, however, that *iar4* mutants contain reduced free IAA content in specific organs or cell types that were not detected at the gross anatomical level employed in our analysis. Despite our inability to detect a reduction in free IAA content, we did observe multiple changes in auxin homeostasis in *iar4* mutants. The vast majority of the IAA in plants is present in a variety of conjugated forms. Enzymes capable of hydrolyzing many of these conjugates are known to exist, suggesting that these forms function to provide a readily accessible and easily regulated source of free

IAA without de novo synthesis. Our analysis of IAA conjugates detected a significant increase in amide-linked IAA-amino acid conjugates in *iar4-3* compared to the wild type. This finding contradicts the hypothesis of LeClere et al. (2004), who speculated that the increased resistance of *iar4-1* seedlings to IAA-Ala may be due to decreased levels of IAA-amino acid conjugates. Rather, the resistance of *iar4* mutants to IAA-amino acid conjugates may be the result of a reduced ability to hydrolyze conjugates, which could account for the elevated levels of IAA conjugates in *iar4* plants as well as IAA deficiency in certain tissues, as suggested by several of our findings. Consistent with this possibility, we find that while high temperature can suppress the slow root growth, auxin resistance, lateral root, and root hair phenotypes of *iar4-3*, it does not suppress the mutant's resistance to IAA-Ala (M. Quint and W.M. Gray, unpublished data; figure 3 in LeClere et al., 2004). Furthermore, we found that IAA-Glu, but not IAA-Asp, conjugates were elevated in *iar4-3* seedlings. Unlike IAA-Glu, IAA-Asp has been shown to be rapidly oxidized to OxIAA-Asp (Ostin et al., 1998), suggesting that IAA-Asp is primarily a component of the IAA catabolic pathway (Tsurumi and Wada, 1986; Tuominen et al., 1994), while IAA-Glu may be stored for later use. The potential hydrolysis of IAA from IAA-Glu is further suggested by the finding that IAA-Glu inhibits Arabidopsis root growth whereas IAA-Asp does not (LeClere et al., 2002).

We also detected increased usage of the Trp-independent IAA biosynthesis pathway in *iar4* seedlings. LeClere et al. (2004) speculated that IAR4 may catalyze the conversion of IPA to indole-3-acetyl-CoA. IPA is an intermediate in the synthesis of IAA from Trp in several plant-associated microbes. IPA is present in Arabidopsis (Tam et al., 2000) and significantly contributes to the IAA pool (Stepanova et al., 2008; Tao et al., 2008). However, our feeding experiments failed to detect a significant difference between *iar4* and control seedlings in the synthesis of IAA from stable isotope-labeled Trp, suggesting that IAR4 does not function in the Trp-dependent IAA biosynthetic pathway. Rather, we detected a significant increase in the utilization of the Trp-independent IAA biosynthetic pathway in *iar4* seedlings. Whether this reflects a direct role for IAR4 in this pathway or represents an attempt to compensate for a possible auxin deficiency is uncertain.

IAR4 encodes a putative E1α-subunit of mitochondrial pyruvate dehydrogenase. Our localization studies with IAR4-GFP plants, together with a previous proteomic study of the mitochondrial proteome (Millar et al., 2001) demonstrate that IAR4 is indeed a mitochondrial protein. The presence of two putative mitochondrial E1α-subunits (*IAR4* and *IAR4L/AT1G59900*) in Arabidopsis raised the possibility that IAR4 may not function as a typical PDC subunit but instead has evolved a novel activity required for maintaining auxin homeostasis. This possibility is supported by the absence of any obvious distortions in downstream

tricitric acid cycle metabolite levels and responses in *iar4-1* mutants, as well as the absence of auxin phenotypes in the *iar4L* single mutant (LeClere et al., 2004). However, our genetic studies strongly support the possibility that these two genes exhibit overlapping function, as at least one of these genes must be present for both pollen and embryo viability. Our finding that *iar4L iar4* pollen is inviable is in agreement with a previous report that antisense expression of a sugar beet (*Beta vulgaris*) E1α-subunit in tobacco (*Nicotiana tabacum*) anther tapetum results in male sterility (Yui et al., 2003). Consistent with a high demand for mitochondrial acetyl-CoA during pollen development, both the number of mitochondria per cell and respiration rates increase significantly during pollen development (Warmke and Lee, 1977; Tadege and Kuhlemeier, 1997). The simplest explanation for the pollen and embryo lethality of *iar4L iar4* double mutants is the presumptive lack of mitochondrial PDC activity. However, this does not preclude the possibility that IAR4 might moonlight as an enzyme involved in some aspect of auxin homeostasis, as previous studies have found that duplications of a variety of genes encoding core metabolic enzymes have led to the evolution of novel enzyme functions (Conant and Wolfe, 2008).

Our understanding of IAA biosynthesis, conjugation, and degradation is far from complete. Precisely how a PDC or PDC-like enzyme might function in auxin homeostasis is unclear. However, our findings that *iar4* mutant phenotypes can be suppressed by increasing endogenous auxin levels together with the changes we observe in IAA conjugate levels and biosynthetic pathway utilization strongly suggest that IAR4 plays an important role in maintaining proper auxin homeostasis. Future studies aimed at elucidating precisely how IAR4 fits into the IAA network may reveal important insight into the control of auxin metabolism as well as potential links to glycolysis.

MATERIALS AND METHODS

Plant Material and Growth Conditions

All Arabidopsis (*Arabidopsis thaliana*) lines employed in this study are in the Col ecotype. Seedlings were grown under sterile conditions on ATS nutrient medium (Lincoln et al., 1990) under long-day lighting conditions. Conditions for the mutagenesis and screen for *eta* mutants have been previously described (Gray et al., 2003).

Map-Based Isolation of the *ETA5/IAR4* Gene

A total of 300 auxin-resistant F2 seedlings from a cross between *eta5-2/iar4-4* and Landsberg *erecta* (L*er*) were used to map the *eta5-2/iar4-4* mutation using simple sequence length polymorphic markers. We initially mapped the *eta5-2/iar4-4* mutation to an interval between markers F21M12 (3.2 Mb) and nga392 (9.8 Mb) (http://www.arabidopsis.org). Markers defining our final mapping interval of approximately 117 kb were CER452019 (5′-CTCTATT-TAACTTAGCAGTC-3′ and 5′-CCTGAAGTCAGCATCAGCTC-3′), which amplifies 201- and 182-bp fragments from Col and L*er*, respectively; and CER459522 (5′-CTGTAGACCAGATACAACTTC-3′ and 5′-TCATGAGTA-

GATATCTAACC-3′), which amplifies 97- and 89-bp products from Col and L*er*, respectively. These and additional markers are available upon request.

Glucuronidase Histochemical Staining

For promotor-GUS studies, a 3.1-kb fragment containing genomic sequence from 1,149-bp upstream of the *IAR4* locus through the third *IAR4* exon 1,960-bp downstream of the ATG start codon was cloned in frame with the GUS coding sequence of pBI101.2 (CLONTECH). Plants were stably transformed using *Agrobacterium tumefaciens*-mediated transformation using standard protocols. Transgenic lines were selected on ATS medium containing 50 mg/L kanamycin. T3 seedlings were stained for GUS activity as previously described (Stomp, 1991).

The HS::AXR3NT-GUS transgene (Gray et al., 2001) was crossed into the *iar4-3* mutant. Six-day-old Col and *iar4-3* seedlings homozygous for the reporter construct were heat shocked for 2 h at 37°C to induce expression of the transgene. Seedlings were then stained immediately or transferred to 20°C medium for the indicated time period and stained for GUS activity (Stomp, 1991). 1-Naphthaleneacetic acid (50 μM) was added during the 20°C incubation where indicated. To account for the difference in steady-state levels of the AXR3NT-GUS protein as shown in Figure 4A and to obtain a similar staining baseline for the degradation assay, Col seedlings in Figure 4B were GUS stained for 480 min and *iar4-3* seedlings were GUS stained for 165 min, respectively. Col seedlings in Figure 4C were GUS stained overnight, and *iar4-3* seedlings were GUS stained for 120 min, respectively.

Microscopy

For pollen staining, anthers were removed from flowers and mounted on microscope slides in one-half times Alexander's solution (Johnson-Brousseau and McCormick, 2004). Viable pollen grains appear dark purple (green walls and densely staining cytoplasm), whereas inviable pollen appear empty (green walls only). To examine developing embryos, siliques were dissected with a 30-gauge needle, cleared overnight in Hoyer's solution (4 g chloral hydrate dissolved in 1 mL 50% glycerol), and visualized on a Nikon Diaphot 200 inverted microscope.

For subcellular localization of IAR4 protein, *IAR4* genomic DNA (from 1,840-bp upstream of the start codon to the end of the coding sequence minus the stop codon) was GATEWAY cloned into pDONR207 and subsequently recombined into the binary vector pMDC107 (Curtis and Grossniklaus, 2003) according to the manufacturer's protocols (Invitrogen). The resulting *IAR4pro*: *IAR4:GFP* construct was stably transformed into Col plants as described above. *IAR4pro:IAR4:GFP* transgenic seedlings were soaked in MitoTracker Orange (Molecular Probes) solution and GFP and MitoTracker fluorescence examined on a Bio-Rad MRC 1024 laser-scanning confocal microscope as previously described (Mano et al., 2002).

IAA Analysis

Extraction of Free IAA and IAA Amino Acid Conjugates

Free IAA content was determined according to Barkawi et al. (2008). To extract IAA-amino acid conjugates, frozen tissue samples were homogenized in 65% isopropanol, 0.2 M imidazole (pH 7) with 10 ng each of [$^{13}C_6$]IAA-Asp and [$^{13}C_6$]IAA-Glu as isotopically labeled internal standards. Homogenization was performed using a Mixermill 3000 (Qiagen) with 3-mm tungsten-carbide beads at 20 Hz for 3 min. The homogenized samples were allowed to equilibrate with the internal standards for 1 h at 4°C, after which they were spun at 10,000g for 5 min. Supernatants were diluted 10× with distilled water to dilute the salt concentration before solid phase extraction. Samples were purified by on-column purification using NH$_2$ (50 mg Versaplate, Varian) and C18 (100 mg PrepSep, Fisher) solid phase extraction columns. Amino columns were first conditioned using 600 μL each of hexane, acetonitrile, distilled water, and 0.2 M imidazole (pH 7), and then twice with 1,600 μL distilled water. The diluted supernatants were loaded on the NH$_2$ columns and allowed to equilibrate for 5 min before being drawn slowly through the column using vacuum. The NH$_2$ columns were then washed with 600 μL each of hexane, ethyl acetate, acetonitrile, and methanol, and the IAA amino acids were eluted 3 times with 0.3 mL 3% formic acid. The C18 columns were conditioned with 1 mL each of methanol and distilled water, and the total NH$_2$ eluates were loaded on the columns and allowed to equilibrate for 5 min before a slight vacuum was applied to draw the samples through. The C18

columns were washed twice with 600 μL distilled water and the IAA amino acids were eluted twice with 300 μL methanol. To methylate the samples before gas chromatography-mass spectrometry (MS) analysis, in a well-ventilated hood, 1 mL ethereal diazomethane was added to each sample and they were immediately placed under a stream of N$_2$ and evaporated to complete dryness. The samples were brought into solution in 25 μL ethyl acetate and analyzed by gas chromatography-MS using selected ion monitoring using a model 6890N GC/5973 Network MS (Agilent Technologies) equipped with an HP-5MS fused-silica capillary column (30 m × 0.25 mm ID, [5%-phenyl]-methylpolysiloxane, 0.25 lm film thickness, Agilent Technologies). The GC injector temperature was set at 280°C and temperature programmed from 70°C (2 min) to 280°C (5 min) at 20°C min^{-1}, with helium as a carrier gas at a flow rate of 1 mL/min. The quadrupole MS was run in EI mode with an electron emission of 70 eV. For both IAA amino acid methyl esters and their isotopically labeled standards, the molecular ions and the base peaks were monitored. For Me-IAA-Asp and Me-[$^{13}C_6$]IAA-Asp, the ions were mass-to-charge ratio (m/z) 130 and 318 and m/z 136 and 324, respectively. For Me-IAA-Glu and Me-[$^{13}C_6$]IAA-Glu, the ions were m/z 130 and 332 and m/z 136 and 338, respectively.

IAA Precursor Feeding

The IAA precursor feeding experiments were modified after Rapparini et al. (2002). In brief, to quantify utilization of Trp-dependent and Trp-independent IAA biosynthetic pathways, seedlings were grown for 10 d at 20°C on vertical petri dishes containing ATS medium. After 10 d they were placed horizontally on a horizontal shaker at 20°C, flooded with 5 mL of 100 μM stable isotope labeled ^{2}H$_5$-Trp (Merck Frosst Canada, MSD Isotopes Div.) and ^{15}N-anthranilate (Icon Services, Inc.) in 10 mM MES (pH 6), and incubated for 24 h. The seedlings were then rinsed, blotted dry, immediately frozen in liquid N$_2$, and stored at −80°C until analyzed for determination of the isotopic enrichment in the endogenous free IAA pool. Extraction and analysis of free IAA was performed as described above.

LITERATURE CITED

Abas L, Benjamins R, Malenica N, Paciorek T, Wisniewska J, Moulinier-Anzola JC, Sieberer T, Friml J, Luschnig C (2006) Intracellular trafficking and proteolysis of the Arabidopsis auxin-efflux facilitator PIN2 are involved in root gravitropism. Nat Cell Biol **8:** 249–256

Barkawi LS, Tam YY, Tillman JA, Pederson B, Calio J, Al-Amier H, Emerick M, Normanly J, Cohen JD (2008) A high-throughput method for the quantitative analysis of indole-3-acetic acid and other auxins from plant tissue. Anal Biochem **372:** 177–188

Chuang HW, Zhang W, Gray WM (2004) *Arabidopsis* ETA2, an apparent ortholog of the human cullin-interacting protein CAND1, is required for auxin responses mediated by the SCF(TIR1) ubiquitin ligase. Plant Cell **16:** 1883–1897

Cohen JD, Slovin JP, Hendrickson AM (2003) Two genetically discrete pathways convert tryptophan to auxin: more redundancy in auxin biosynthesis. Trends Plant Sci **8:** 197–199

Conant GC, Wolfe KH (2008) Turning a hobby into a job: how duplicated genes find new functions. Nat Rev Genet **9:** 938–950

Curtis MD, Grossniklaus U (2003) A gateway cloning vector set for high-throughput functional analysis of genes in planta. Plant Physiol **133:** 462–469

Delarue M, Prinsen E, Onckelen HV, Caboche M, Bellini C (1998) Sur2 mutations of Arabidopsis thaliana define a new locus involved in the control of auxin homeostasis. Plant J **14:** 603–611

Dharmasiri N, Dharmasiri S, Weijers D, Lechner E, Yamada M, Hobbie L, Ehrismann JS, Jurgens G, Estelle M (2005) Plant development is

regulated by a family of auxin receptor F box proteins. Dev Cell **9:** 109–119

Goddijn OJ, de Kam RJ, Zanetti A, Schilperoort RA, Hoge JH (1992) Auxin rapidly down-regulates transcription of the tryptophan decarboxylase gene from Catharanthus roseus. Plant Mol Biol **18:** 1113–1120

Gray WM, Kepinski S, Rouse D, Leyser O, Estelle M (2001) Auxin regulates SCF(TIR1)-dependent degradation of AUX/IAA proteins. Nature **414:** 271–276

Gray WM, Muskett PR, Chuang HW, Parker JE (2003) *Arabidopsis* SGT1b is required for SCF(TIR1)-mediated auxin response. Plant Cell **15:** 1310–1319

Gray WM, Ostin A, Sandberg G, Romano CP, Estelle M (1998) High temperature promotes auxin-mediated hypocotyl elongation in Arabidopsis. Proc Natl Acad Sci USA **95:** 7197–7202

Johnson-Brousseau SA, McCormick S (2004) A compendium of methods useful for characterizing Arabidopsis pollen mutants and gametophytically-expressed genes. Plant J **39:** 761–775

Johnston ML, Luethy MH, Miernyk JA, Randall DD (1997) Cloning and molecular analyses of the Arabidopsis thaliana plastid pyruvate dehydrogenase subunits. Biochim Biophys Acta **1321:** 200–206

Kramer EM, Bennett MJ (2006) Auxin transport: a field in flux. Trends Plant Sci **11:** 382–386

LeClere S, Rampey RA, Bartel B (2004) IAR4, a gene required for auxin conjugate sensitivity in Arabidopsis, encodes a pyruvate dehydrogenase E1alpha homolog. Plant Physiol **135:** 989–999

LeClere S, Tellez R, Rampey RA, Matsuda SP, Bartel B (2002) Characterization of a family of IAA-amino acid conjugate hydrolases from Arabidopsis. J Biol Chem **277:** 20446–20452

Lincoln C, Britton JH, Estelle M (1990) Growth and development of the axr1 mutants of *Arabidopsis*. Plant Cell **2:** 1071–1080

Ljung K, Hull AK, Kowalczyk M, Marchant A, Celenza J, Cohen JD, Sandberg G (2002) Biosynthesis, conjugation, catabolism and homeostasis of indole-3-acetic acid in Arabidopsis thaliana. Plant Mol Biol **49:** 249–272

Luethy MH, Miernyk JA, Randall DD (1995) The mitochondrial pyruvate dehydrogenase complex: nucleotide and deduced amino-acid sequences of a cDNA encoding the Arabidopsis thaliana E1 alpha-subunit. Gene **164:** 251–254

Mano S, Nakamori C, Hayashi M, Kato A, Kondo M, Nishimura M (2002) Distribution and characterization of peroxisomes in Arabidopsis by visualization with GFP: dynamic morphology and actin-dependent movement. Plant Cell Physiol **43:** 331–341

Masucci JD, Schiefelbein JW (1996) Hormones act downstream of TTG and GL2 to promote root hair outgrowth during epidermis development in the *Arabidopsis* root. Plant Cell **8:** 1505–1517

Millar AH, Sweetlove LJ, Giege P, Leaver CJ (2001) Analysis of the Arabidopsis mitochondrial proteome. Plant Physiol **127:** 1711–1727

Mooney BP, Miernyk JA, Randall DD (2002) The complex fate of alpha-ketoacids. Annu Rev Plant Biol **53:** 357–375

Ostin A, Kowalyczk M, Bhalerao RP, Sandberg G (1998) Metabolism of indole-3-acetic acid in Arabidopsis. Plant Physiol **118:** 285–296

Paciorek T, Zazimalova E, Ruthardt N, Petrasek J, Stierhof YD, Kleine-Vehn J, Morris DA, Emans N, Jurgens G, Geldner N, et al (2005) Auxin inhibits endocytosis and promotes its own efflux from cells. Nature **435:** 1251–1256

Quint M, Gray WM (2006) Auxin signaling. Curr Opin Plant Biol **9:** 448–453

Quint M, Ito H, Zhang W, Gray WM (2005) Characterization of a novel temperature-sensitive allele of the CUL1/AXR6 subunit of SCF ubiquitin-ligases. Plant J **43:** 371–383

Rapparini F, Tam YY, Cohen JD, Slovin JP (2002) Indole-3-acetic acid metabolism in Lemna gibba undergoes dynamic changes in response to growth temperature. Plant Physiol **128:** 1410–1416

Sauer M, Balla J, Luschnig C, Wisniewska J, Reinohl V, Friml J, Benkova E (2006) Canalization of auxin flow by Aux/IAA-ARF-dependent feedback regulation of PIN polarity. Genes Dev **20:** 2902–2911

Staswick PE, Serban B, Rowe M, Tiryaki I, Maldonado MT, Maldonado MC, Suza W (2005) Characterization of an *Arabidopsis* enzyme family that conjugates amino acids to indole-3-acetic acid. Plant Cell **17:** 616–627

Stepanova AN, Robertson-Hoyt J, Yun J, Benavente LM, Xie DY, Dolezal K, Schlereth A, Jurgens G, Alonso JM (2008) TAA1-mediated auxin biosynthesis is essential for hormone crosstalk and plant development. Cell **133:** 177–191

Stomp A-M (1991) Histochemical localization of β-glucuronidase. *In* SR Gallagher, ed, GUS Protocols. Academic Press, London, pp 103–113

Tadege M, Kuhlemeier C (1997) Aerobic fermentation during tobacco pollen development. Plant Mol Biol **35:** 343–354

Tam YY, Epstein E, Normanly J (2000) Characterization of auxin conjugates in Arabidopsis: low steady-state levels of indole-3-acetyl-aspartate, indole-3-acetyl-glutamate, and indole-3-acetyl-glucose. Plant Physiol **123:** 589–596

Tao Y, Ferrer JL, Ljung K, Pojer F, Hong F, Long JA, Li L, Moreno JE, Bowman ME, Ivans LJ, et al (2008) Rapid synthesis of auxin via a new tryptophan-dependent pathway is required for shade avoidance in plants. Cell **133:** 164–176

Tsurumi S, Wada S (1986) Dioxindole-3-acetic acid conjugates formation from indole-3-acetylaspartic acid in Vicia seedlings. Plant Cell Physiol **27:** 1513–1522

Tuominen H, Ostin A, Sandberg G, Sundberg B (1994) A novel metabolic pathway for indole-3-acetic acid in apical shoots of *Populus tremula* (L.) × *Populus tremuloides* (Michx.). Plant Physiol **106:** 1511–1520

Walz A, Park S, Slovin JP, Ludwig-Muller J, Momonoki YS, Cohen JD (2002) A gene encoding a protein modified by the phytohormone indoleacetic acid. Proc Natl Acad Sci USA **99:** 1718–1723

Warmke HE, Lee SLJ (1977) Mitochondrial degeneration in Texas cytoplasmic male-sterile corn anthers. J Hered **68:** 213–222

Woodward AW, Bartel B (2005) Auxin: regulation, action, and interaction. Ann Bot (Lond) **95:** 707–735

Yui R, Iketani S, Mikami T, Kubo T (2003) Antisense inhibition of mitochondrial pyruvate dehydrogenase E1alpha subunit in anther tapetum causes male sterility. Plant J **34:** 57–66

Zhang W, Ito H, Quint M, Huang H, Noel LD, Gray WM (2008) Genetic analysis of CAND1-CUL1 interactions in Arabidopsis supports a role for CAND1-mediated cycling of the SCFTIR1 complex. Proc Natl Acad Sci USA **105:** 8470–8475

Zhao Y, Christensen SK, Fankhauser C, Cashman JR, Cohen JD, Weigel D, Chory J (2001) A role for flavin monooxygenase-like enzymes in auxin biosynthesis. Science **291:** 306–309